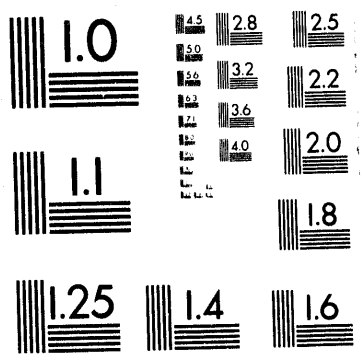
1.0
1.1
1.25
1.4
1.6
1.8
2.0
2.2
2.5
2.8
3.2
3.6
4.0
4.5
5.0
5.6
6.3
7.1
8.0
9.0

1 of 1

To be published in the Proceedings of the
IV International Conf. on Calorimetry in High Energy Physics

BNL-49806

IONIZATION EM CALORIMETERY WITH ACCORDION ELECTRODES AND LIQUID KRYPTON OR ARGON*

Veljko Radeka
Brookhaven National Laboratory, Upton, NY 11973 USA

DISCLAIMER

November 1993

*This research was supported by the U.S. Department of Energy:
Contract No. DE-AC02-76CH00016.

Ionization EM Calorimetry with Accordion Electrodes and Liquid Krypton or Argon

Veljko Radeka
Brookhaven National Laboratory, Upton, NY 11973

Abstract

The results of a study and tests of a liquid krypton/argon electromagnetic calorimeter with accordion electrode structure are briefly summarized. This includes the calorimeter response to electrons and muons, energy, pointing and timing resolution, and a measurement by multiple sampling. The electrode layout with fine segmentation is illustrated.

1. Introduction

A steady progression of advances has brought the liquid ionization calorimetry to the forefront of techniques for high precision calorimetry at hadron colliders. Liquid argon (LAr) has been used in several large calorimeters[1,2,3] where the long term stability of the response has been well established. In the development of the calorimeter for the HELIOS (NA34) experiment, it was understood that the limit to the speed of response was determined by the charge transfer from the electrodes into the amplifier and by the signal-to-noise ratio, and not by the electron drift time.[4,5] This led also to the development and use of preamplifiers operated at the electrodes in the liquid at low temperatures. The accordion electrode concept, introduced by D. Fournier and developed by the RD3 collaboration, made feasible high speed EM calorimetry with fine segmentation into small towers or strips.[6,7,8] A projective accordion calorimeter was demonstrated with an energy resolution of $9-10\%/\sqrt{E}$ up to 300 GeV with a small constant term and a fast response (impulse response of 20 ns). Independently, the use of liquid krypton (LKr) was investigated to obtain an even better energy resolution.[9,10,11] This work resulted in the development of quasi-homogenous prototype calorimeters with very thin electrodes for the KEDR detector[9,11] and for the NA48 experiment.[10] A quasi-homogenous calorimeter could potentially achieve the best energy resolution (in the 3-4% range), but the length (25 X_0 ~ 120 cm) and the quantity of LKr are disadvantages for a large barrel calorimeter in collider experiments.

A sampling calorimeter with an accordion electrode structure and a relatively high sampling fraction (in the range of 1/5 to 1/3) satisfies best so far many diverse considerations such as: a compact size; minimal shower width; energy, pointing and timing resolution; fine segmentation; electrode capacitance and signal-to-noise ratio. A study of this type of calorimeter with LAr and with LKr was performed at the BNL Alternating Gradient Synchroton (AGS). The results are described in some detail in Ref. 12. A study of the timing properties of this device with LKr has been reported recently.[13] A study of amplitude and timing measurements in this calorimeter by multiple sampling of signals has also been completed.[14] The aim of this work has been to bring the energy resolution of such an EM accordion calorimeter into the range of about $6\%/\sqrt{E}$.

In this paper some of the results of these studies are highlighted and summarized. The concept for the electrode structure and segmentation in the EM calorimeter design for the GEM experiment[15] is also presented. The results discussed here were obtained by the EM Liquid Ionization Calorimetry Collaboration of GEM.[16]

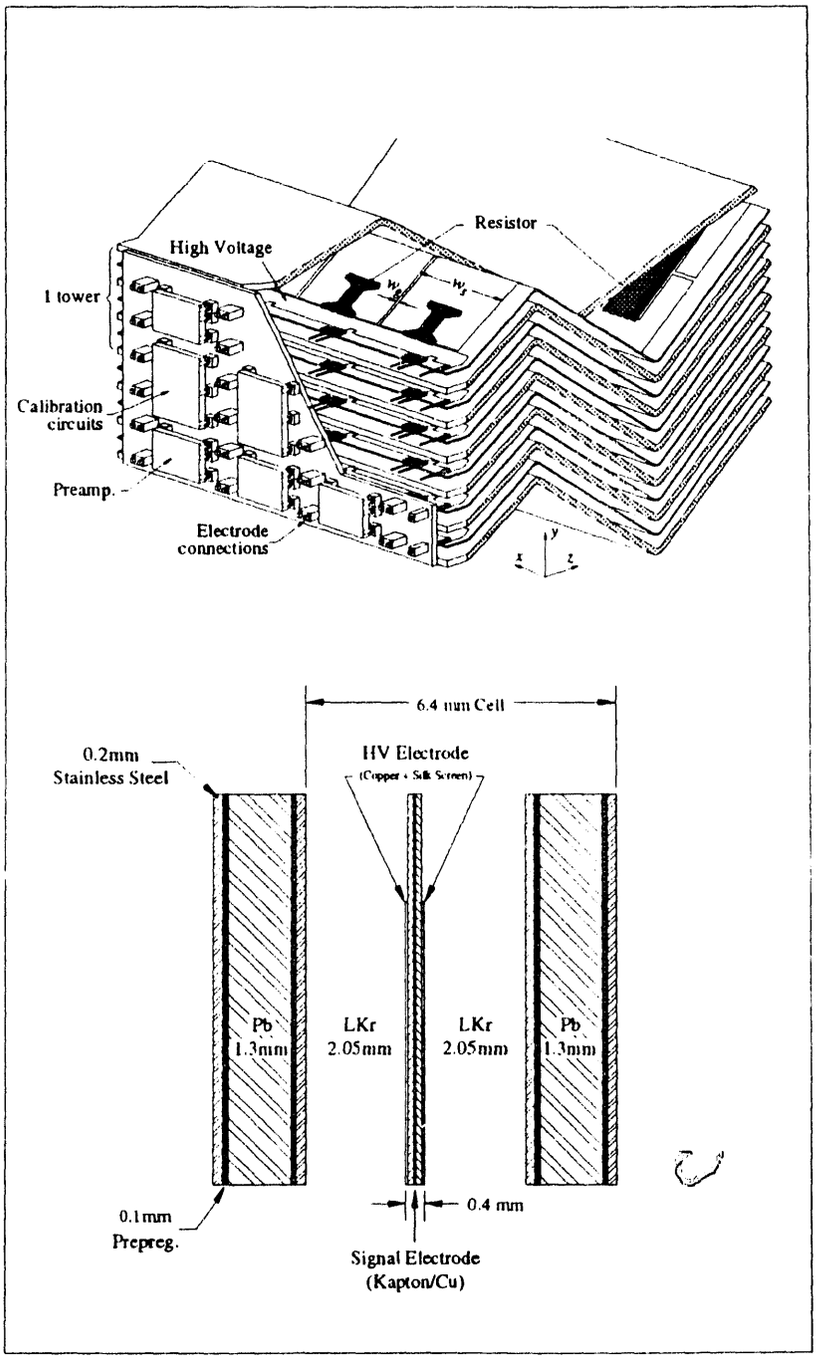

Fig. 1 Accordion absorber/electrode structure. Signal electrodes are connected to the preamplifiers by the pin connections on the motherboard. A calorimeter tower is defined in width by the artwork on the electrodes and in height by the grouping of 3 readout electrodes. The tower dimensions are: $w_g + w_s = 25$ mm, the gap between adjacent strip electrode metalizations $w_g = 0.5$ mm, and the tower height 27.0 mm. The absorber plates are made of 1.3 mm lead with 0.2 mm stainless steel. Shaded areas indicate film resistors. The sampling fraction $\eta_s = 0.325(0.228)$ for this electrode structure with LKr (LAr). The calorimeter is subdivided in depth into two sections $6\ X_0 + 18\ X_0 = 24\ X_0$ (LKr), and $5\ X_0 + 15\ X_0 = 20\ X_0$ (LAr)

2. Test Accordion Calorimeter with LAr and LKr

A cutaway view of the accordion electrode structure showing the absorber and signal electrodes, electrical connections, and internal electronics is shown in Fig. 1. The signal electrode consists of copper clad kapton sheets, etched into 2.5 cm wide strips. This defines the horizontal dimension of the readout tower (the bends of the accordion are in the vertical direction). One tower consists of three signal electrodes (cells) connected together which defines the vertical tower dimension of 2.7 cm. Longitudinally, the electrodes are subdivided into two sections $6\ X_0 + 18\ X_0 = 24\ X_0$ (LKr), i.e., $5\ X_0 + 15\ X_0 = 20\ X_0$ (LAr).

The preamplifier and the calibration circuits are located as close as possible to the signal electrodes and are operated at LKr or LAr temperatures. Printed circuit motherboards containing the preamplifiers and calibration circuits are mounted at both ends of the electrode stack for front and back sections. The readout electronics and the calibration pulse generator are shown schematically in Fig. 2. The preamplifiers (BNL design IO583B) use junction field-effect transitors (JFETs) which are radiation hard and can operate in LAr (LKr) and are made by InterFET Corp.[17] The signals from the preamplifiers followed by an intermediate amplifier, are received in the counting room by Variable Gain Amplifiers (VGA). The signals are split into two paths, for recording of individual channels and for forming on-

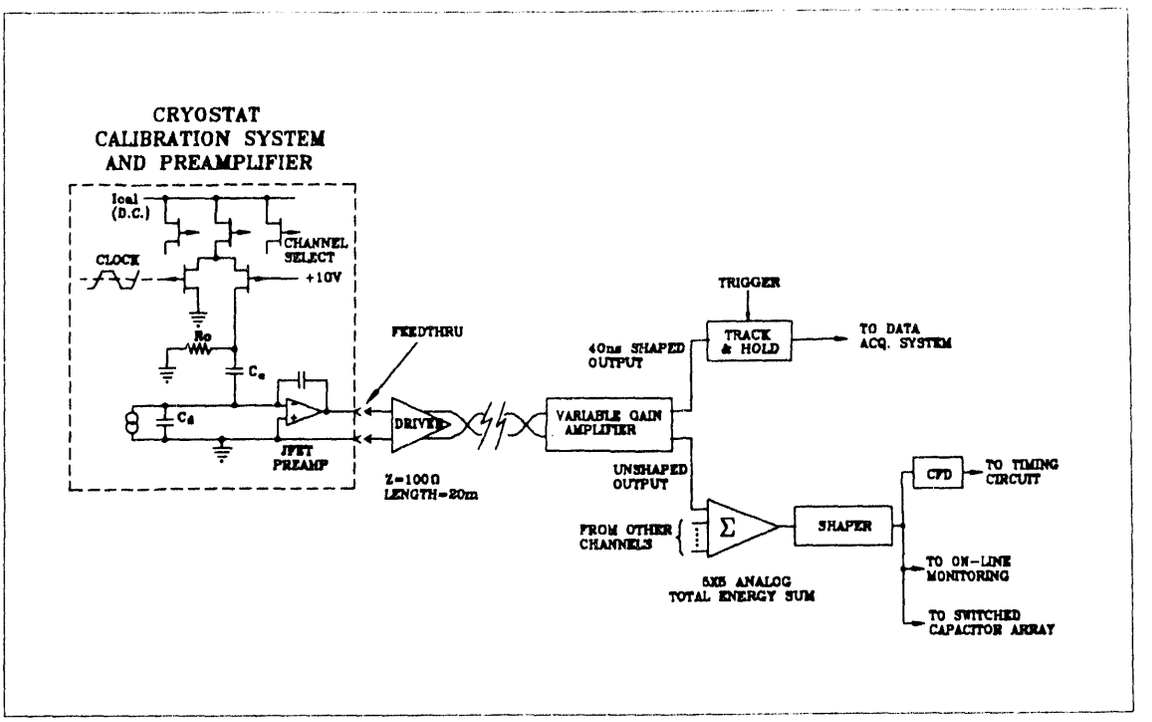

Fig. 2 Electronic readout chain for the calorimeter. The calibration pulse is generated *in situ* by switching off a known current by a clock pulse for the selected channel. The total energy linear sum is provided for online monitoring (e.g., waveforms in Fig. 3) and for measurements by multiple sampling, Fig. 7. The gain of all channels is equalized in computer controlled variable gain amplifiers by the calibration system.

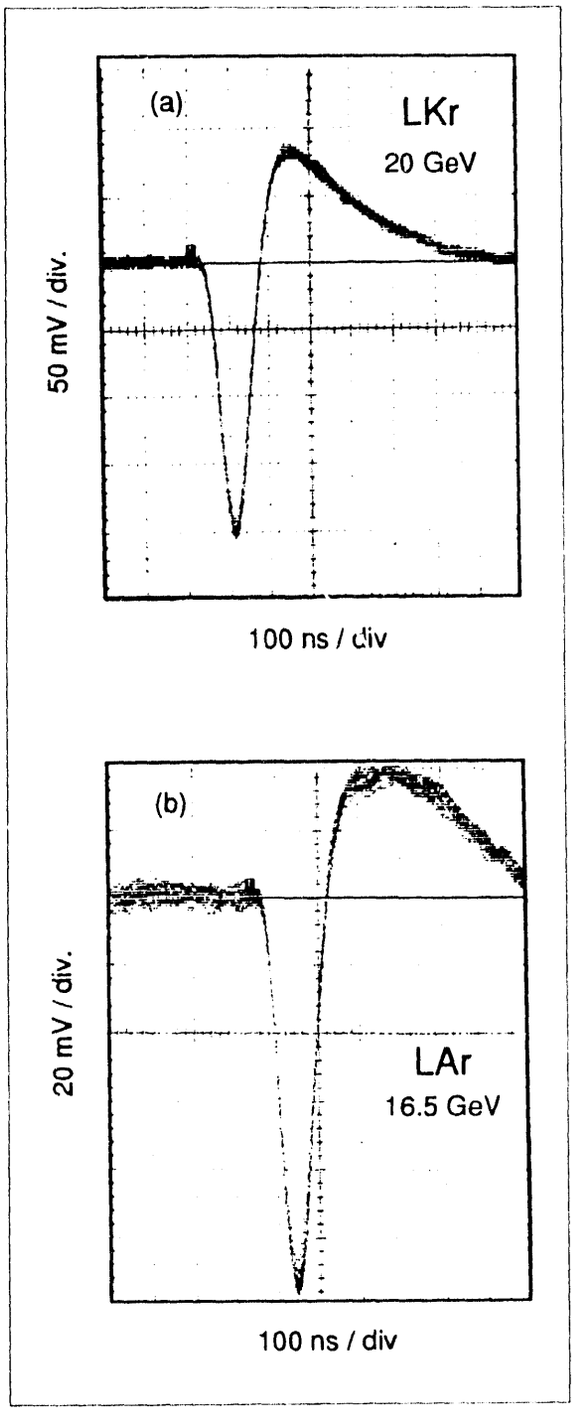

Fig. 3 Online signal waveforms from the calorimeter with Krypton (a) and Argon (b). The signals were obtained from an online sum of 7 x 7 towers (~100 channels) around the beam. The peaking time of the bipolar impulse response was t_m = 40 ns. The electronic gain of all channels was equalized using the calibration system. (a) represents 110 events from 20 GeV e^- beam stored by a digital oscilloscope, whereas (b) represents a total of 50 events from 16.5 GeV e^- beam. Waveforms for LKr were acquired at 1.5 kV, and for LAr at 1.75 kV (the amplifier gain was different in the two cases). The second lobe of the waveform from LKr shows evidence of electron attachment, as discussed in Ref. 12. These traces indicate a high signal-to-noise ratio, and very good energy and timing resolutions, before any corrections. The higher signal-to-noise ratio of LKr is apparent. The signal in LKr is about 1.6 times larger.

line sums (e.g., from the front and back sections of the calorimeter). The gain control of individual channels in the VGAs is carried out through an on-board microprocessor which is interfaced to the main data acquisition system. The calibration system allows equalization of gains to a precision of ~ 0.2%. The sums were used for on-line monitoring, for timing resolution studies and for the studies of signal recording by multiple sampling.

The tests were performed first with LAr and then with LKr. LKr is more sensitive to contamination than LAr due to some electronegative impurities that may remain active at 123 K but not at 90 K. Contamination and purification questions are discussed in Ref. 12. Data in these tests were obtained with 5, 10, 15 and 20 GeV/C electrons. Muon data were taken at 15 GeV/C momentum.

A more detailed description of the calorimeter module, the readout electronics, the calibration system, the cryogenics and purification system and of the experimental setup, is given in Ref. 12.

3. Experimental Results

3.1 Calorimeter Response

Fig. 3 displays the shaped signals from the calorimeter observed with LKr and LAr respectively. The signal waveforms displayed are the total energy sums of 7×7 towers used for monitoring purposes. Multiple consecutive events were stored in a digital oscilloscope. The superposed waveforms provide a useful indication of the energy and timing resolution before any corrections, of the electronic noise, and of any coherent or pickup noise. The waveforms were recorded with the oscilloscope triggered by the electron trigger. The shape of the waveforms also provides an indication of the presence of impurities which cause electron attachment and a reduction in the electron lifetime.[12] The relative loss of signal, due to the electron attachment, is much smaller at short integration times (20-40 ns) used in fast calorimetry than for integration time equal to the electron drift time.

Fig. 4 shows the measured pulse height as a function of high voltage over the interelectrode gap of 2.05 mm for LKr and LAr. The signals were normally processed with an integration time of 40 ns. We also used an integration time of 2 μs for the measurement with LAr in order to observe the total induced charge. The slope dQ/dV is higher at short shaping times than at 2 μs, due to the dependence of the electron drift velocity on the electric field. With LKr, a large signal is seen even at quite low voltages due to the high electron mobility at low electric fields.

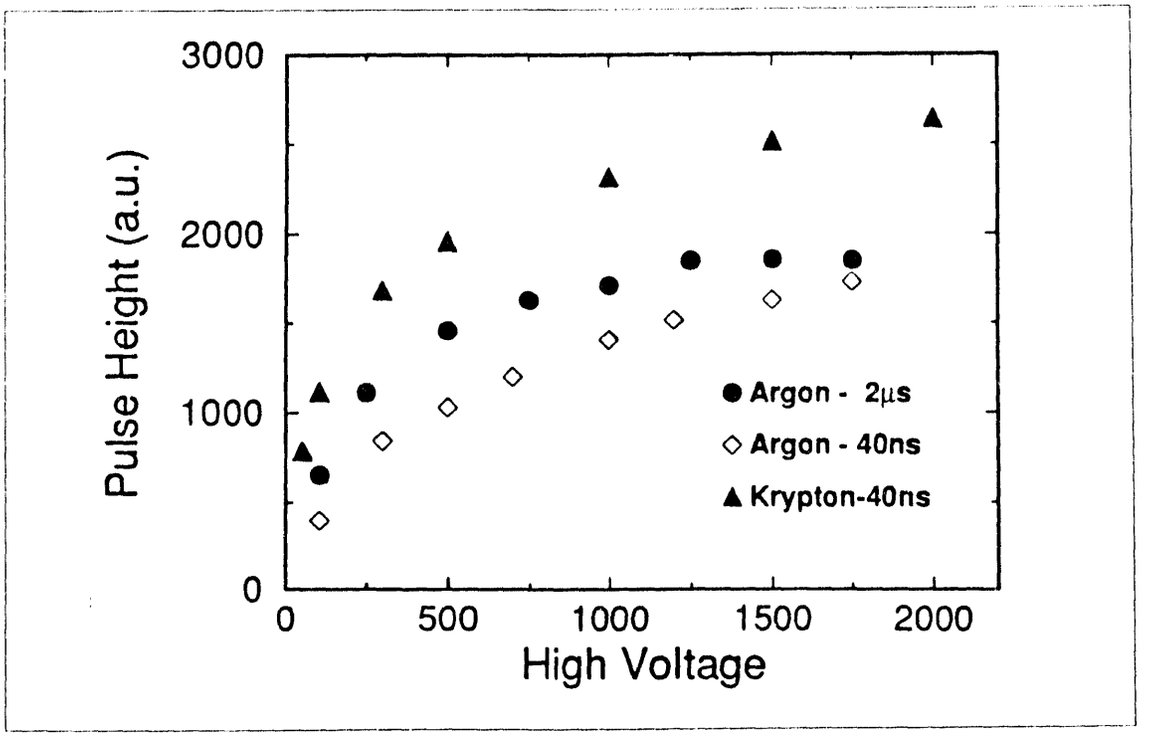

Fig. 4 Pulse height in the calorimeter plotted as a function of the high voltage applied to the electrodes. The open diamond points were taken for an integration time of 40 ns with liquid argon. The full circles were taken with liquid argon with 2 μs integration time (not normalized to the data for 40 ns). Triangles are points for liquid krypton with 40 nsec integration time.

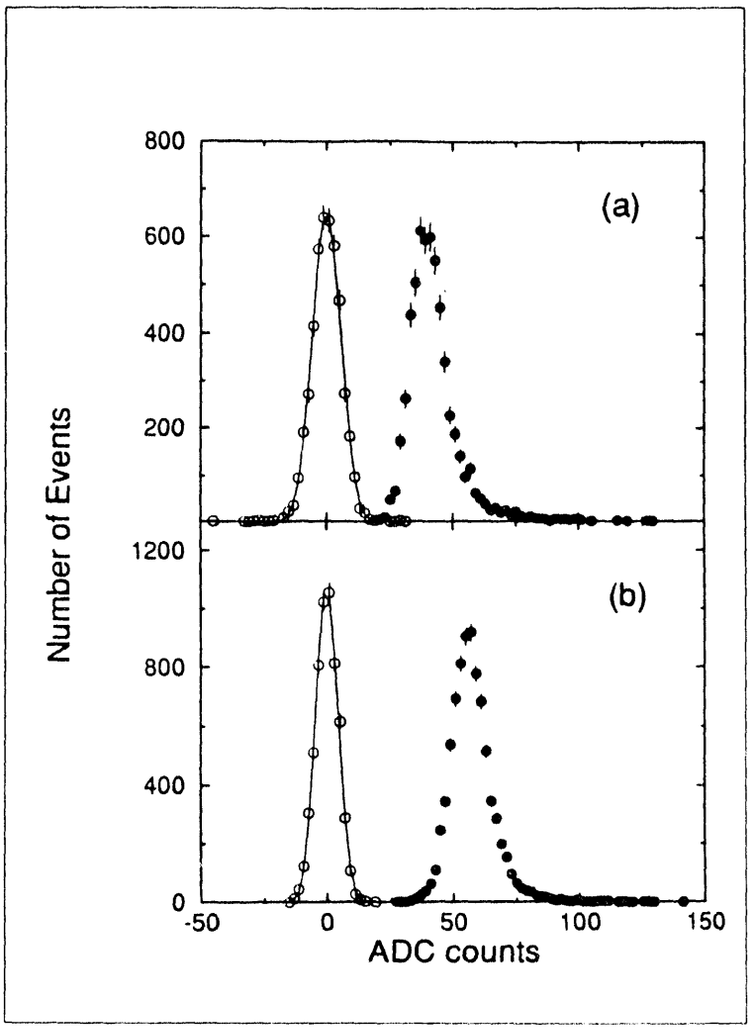

Fig. 5 Muon response of the calorimeter with (a) liquid argon and (b) liquid krypton for 2×1 towers. The pedestals for both runs are shown as open circles. The data for LAr were taken at 1.75 kV. The data for LKr were taken at 1.5 kV and prior to purification of the liquid (After purification and at 2 kV the response from LKr increased 1.1 times.).

The calorimeter muon response is displayed in Fig. 5 for LAr and LKr. The muon energy was defined as the energy deposited in 2×1 towers, and the active length of the liquid in the test calorimeter in Fig. 1 was 29.6 cm. The pulse height for LKr is ~ 1.5 times larger. The electronic noise with LKr is ~ 30% lower, since the noise in Si JFETs has a broad minimum at ~ 120 K. The so called "e/μ ratio" (the ratio of signal charge for electrons and muons for a given amount of energy lost in the calorimeter) for LKr and LAr was found to be 0.75 ± 0.04 and 0.89 ± 0.05, respectively.

3.2 Energy Resolution

The energy resolution was determined from measurements at beam momenta of 5, 10, 15 and 20 GeV/C. The beam size was defined to be 2.5×5 cm^2. The amount of inactive material in front of the active region was 1.5 X_0. The correction for this was based entirely on the ratio of energies in the front and back sections of the calorimeter. The only other correction necessary for the calorimeter response is due to the variation in the vertical direction (across accordion bends), which amounts to about 0.33%. Both corrections were made

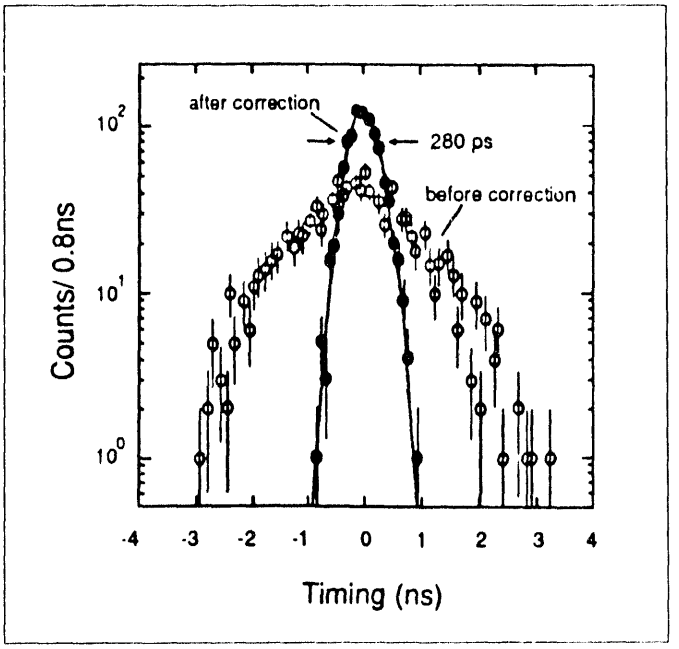

Fig. 6 Distribution of time signals from the sum of 5×5 towers (50 channels) measured at the output of the timing discriminator (open circles). Distribution of time signals after correction for timing differences in individual channels (due to different delays in 20 meter long transmission lines). The start signal to the TDC is determined by the beam counter closest to the calorimeter.

using calorimeter information only. It was found that the response was linear to 0.1%. The energy resolution was fitted to the function,

$$\frac{\sigma_E}{E} = a \oplus \frac{b}{\sqrt{E}} \oplus \frac{c}{E} \quad . \tag{1}$$

The values of the parameters for LKr are a = (0.0 ± 0.2)%, b = (6.72 ± 0.04)% $\sqrt{\text{GeV}}$, and c = 80 MeV for 5 × 5 towers. The data points are shown in Fig. 8 as single sample measurements. These results are for 5 × 5 towers, where 99% of the shower energy is contained. In 3 × 3 towers, 92% of the shower energy is contained, and the resolution is degraded by a factor of ~ 1.09. The Moliere radius for the calorimeter in Fig. 1 with LKr is ~ 3.9 cm. For LAr, a = (0.0 ± 0.2)%, b = (7.7 ± 0.2)% $\sqrt{\text{GeV}}$, and c = 180 MeV. The values for the stochastic term b are in agreement to within ± 0.1% with GEANT simulations of this calorimeter.

3.3 Pointing Resolution

The accordion electrode geometry provides interpolation to determine the position of the shower in the vertical direction by the center of gravity of the signals. Unlike the interleaved towers in the vertical direction, the towers have discrete boundaries in the horizontal direction, which require a correction for the non-linear response of the position information derived from the center of gravity. With the position information from the front and back sections, the angle of electron incidence was found with an angular resolution of (54 ± 0.5) mrad $/\sqrt{E}$ and (53 ± 0.5) mrad $/\sqrt{E}$ for the horizontal and vertical coordinates respectively, with LKr. This result agrees with the Monte Carlo simulation which gives an average resolution of 54 mrad $/\sqrt{E}$.

3.4 *Timing Resolution*

The signal waveforms in ionization calorimeters are very uniform and have very low fluctuations due to a large number of electrons produced (typically $\geq 3 \times 10^6$ e/GeV). This is illustrated by the very narrow spread of the waveforms in Fig. 3 at the zero crossing. Timing resolution studies[13] have shown that, as expected, the timing resolution is very good, and limited at very low energies by the signal-to-noise ratio. Some of the results are given in Table I. The timing measurements can be performed by a simple constant fraction discriminator,[18] as illustrated in Fig. 6. This simple method is limited principally by the differences in transmission line (cable) delays among individual channels for a large calorimeter area. Even without corrections, this simple measurement is sufficient for assignment of events to bunch crossings in hadron colliders. With corrections, the resolution for individual channels allows the assignment of energy depositions as low as 200 MeV, which is of interest for detection of isolated leptons.

Table I

Summary of Results

(Accordion with 1.3 mm lead + 2×0.2 mm stainless steel absorber electrodes)

E [GeV]

	LAr	LKr
Energy resolution $\frac{\sigma_E}{E}$	$7.7\%/\sqrt{E}$	$6.6\%/\sqrt{E}$
Position resolution σ^x_{FB}	-	$6.2mm/\sqrt{E}$
σ^y_{FB}	-	$54mrad/\sqrt{E}$
Pointing resolution σ^x_{FB}	-	$6.0mm/\sqrt{E}$
σ^y_{FB}	-	$53\ mrad/\sqrt{E}$
Timing resolution (5 × 5 towers)	9 GeV ns/E	4.15 GeV ns/E
Timing resolution 1 tower	1.8 GeV ns/E	0 8 GeV ns/E
Peak current/Energy in response to electrons	2.5 μA/GeV	4.2 μA/GeV
Peak Current in response to muons	0.91 μA	1.47 μA
Electronic noise in 5 × 5 towers σ_E(el)	180 MeV	80 MeV

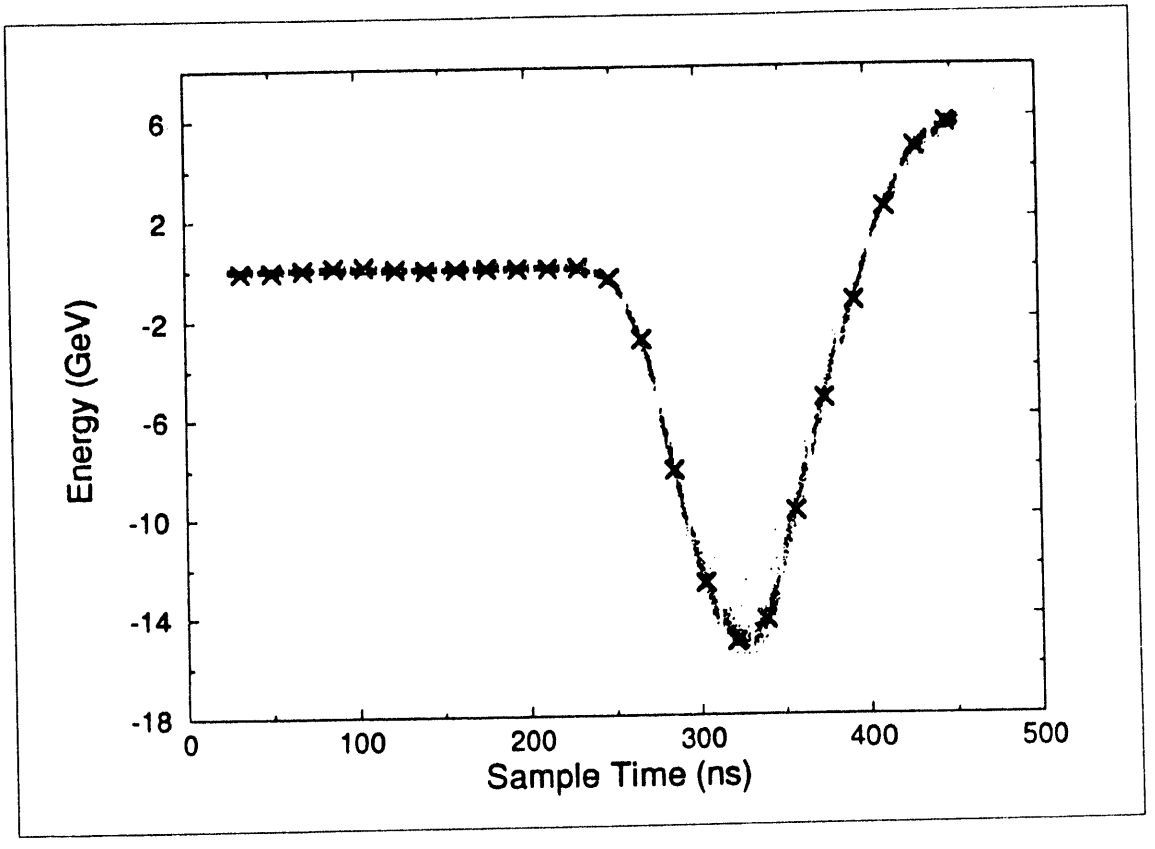

Fig. 7 Signal measurement by multiple sampling. The data were obtained from the sums of front and back sections of 5×5 towers of the calorimeter (50 channels), and are shown superposed from many waveforms. For any particular waveform, a set of samples (indicated by x) were taken at 18 ns intervals. Because the beam in this test enters the calorimeter at random times with respect to the sampling clock, the superposition of many samples gives a complete picture of the waveform.

4. Signal Measurement by Multiple Sampling

The measurements of calorimeter signals by multiple sampling were designed in our tests to emulate the type of data that will be available from a calorimeter operating at a future hadron-hadron collider with a short spacing between bunch crossings (16 to 25 ns). Data have been collected with 18 ns sample spacing on waveforms from individual calorimeter cells and from analog sums of 5×5 towers. Data taken at 15 GeV/C by the sampling system superposed over many waveforms are shown in Fig. 7. For any particular waveform, a set of samples as indicated by crosses were recorded. A continuous waveform emerges in this figure since the beam particles are not synchronized with the sampling clock. A detailed theoretical study of multiple sampling of liquid ionization calorimetry signals has recently been reported.[19] The data were processed using the method of optical filtering, which allows optimization of the filter weighting function with respect to the electronic noise and event pileup, by appropriate weighting of the samples. A detailed analysis of the energy and

timing resolution as a function of the number of samples and the sampling pattern has been performed.[14]

Some results on energy resolution measurements with LKr are shown in Fig. 8, along with more conventional single sample measurements at the peak of the waveform. In the case of 5 samples, every other of the original 18 ns samples were used corresponding to a sampling period of 36 ns. This appears to be sufficient for a peaking time of the system impulse response of ~ 40 ns, as there is no degradation in the energy resolution compared to using 9 samples. A conclusion of these studies is that 4 to 5 samples have to be retained from all the samples in the pipeline memory, to determine the energy and the time origin of an incident particle. With optimal filtering (optimal weighting of samples) the noise in the sum signal of 5×5 towers was reduced from 80 MeV to 37 MeV as expected from the analysis (the resulting weighting function in this case is broader than that of the hardware filter alone). Extraction of the timing information from this data is also reported in Ref. 14.

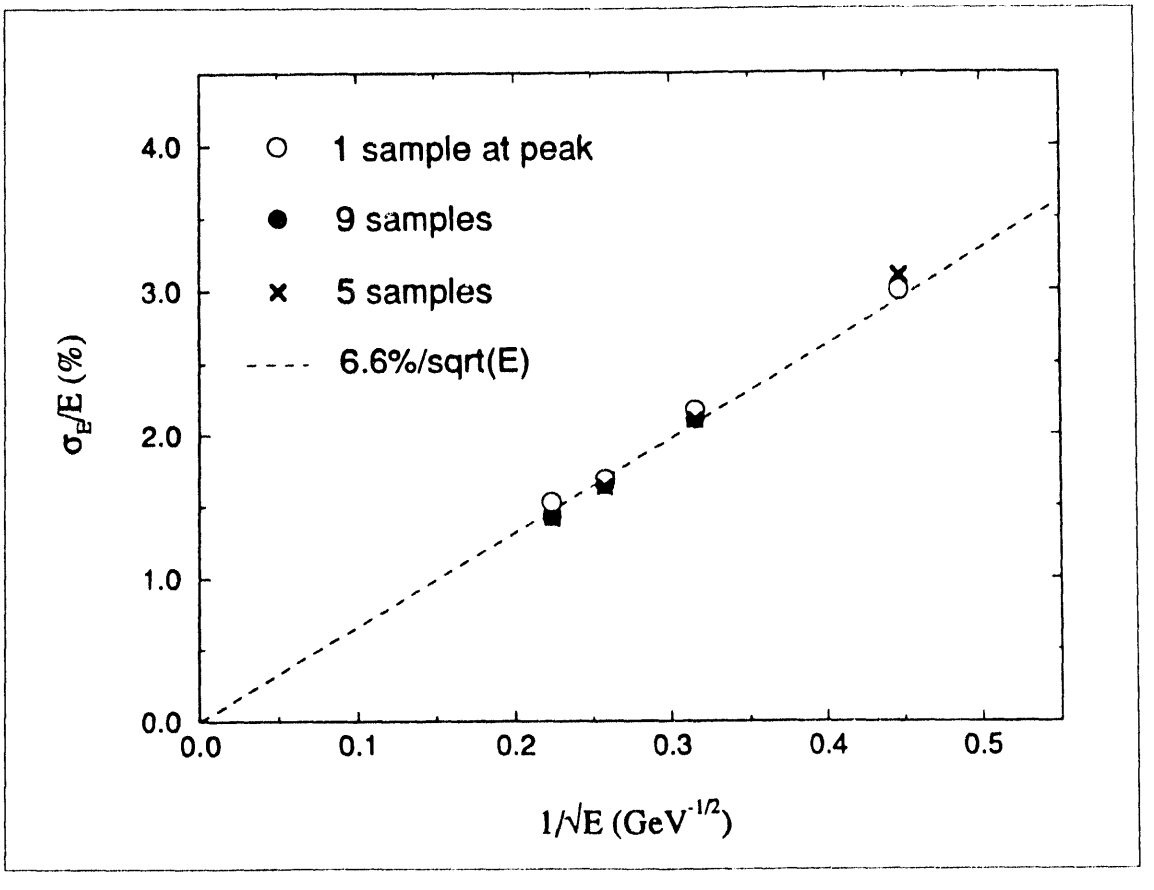

Fig. 8 Energy resolution vs electron energy from the time-sampled data for LKr derived from 9 and 5 asynchronous samples, and compared with single sample measurements at the peak of the waveform. The dashed line is a linear fit to the time-sampled data of the form $\sigma_E / E = b / \sqrt{E}$, with b = 6.6%. A value b = 6.7% was obtained from a GEANT simulation of this calorimeter.

5. EM Calorimeter Configuration for GEM

The design of the accordion EM calorimeter for GEM was optimized for the best energy, position, angular resolution and jet rejection. This optimization involved principally, but not only, the choice of the absorber thickness, the sampling medium (LKr), transversal and longitudinal segmentation and the massless gap. Accordion electrodes lend themselves particularly well to imaginative segmentation patterns while keeping a number of connections to a minimum. The transverse and longitudinal segmentation of the GEM barrel EM calorimeter is shown in Fig. 9. The 6×6 towers covering $\Delta\eta \times \Delta\phi = 0.16 \times 0.16$ also represent an EM trigger tower (this is followed by 2×2 hadron towers covering the same solid angle). The fine strips in the first EM layer match the trigger towers in ϕ while providing jet rejection and pointing in η. This arrangement contains the same number of channels in each longitudinal section. The transverse segmentation and the depth of the first layer (strips) are determined by the need to separate showers.

The three longitudinal subdivisions were determined by the requirements to achieve the best possible angular resolution and hadron rejection. To correct for the energy loss in the material in front of the active calorimeter region, a "massless gap" is incorporated into the front part of the first longitudinal section.

The electrode structure and the connections are shown in Fig. 10. As compared to Fig. 1, with square towers in the first layer, the distinction is in the artwork and connections of the strips, while the readout board with preamplifiers remains essentially the same.

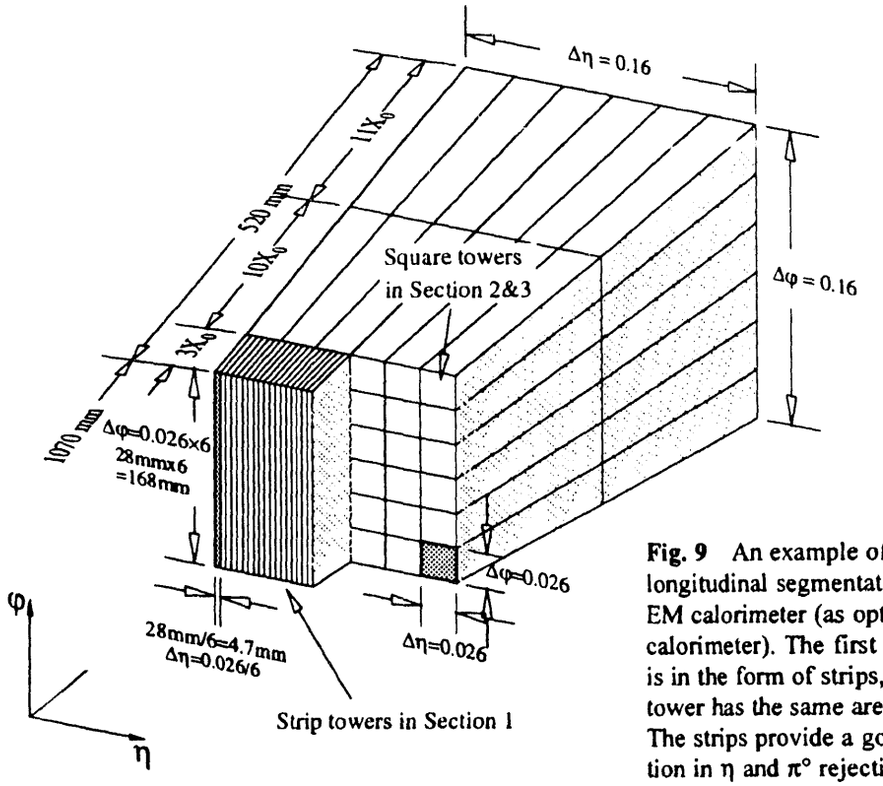

Fig. 9 An example of transverse and longitudinal segmentation of an accordion EM calorimeter (as optimized for the GEM calorimeter). The first longitudinal section is in the form of strips, where each strip tower has the same area as a square tower. The strips provide a good pointing resolution in η and π^0 rejection.

A more detailed description, than possible here, of optimization of various parameters (absorber thickness and calorimeter depth, massless gap, projective accordion bending angles, etc.) is given in Ref. 15 and 20. These simulations show that by reducing the lead thickness in the absorber electrode from 1.3 mm, used in the calorimeter, to 1 mm in the GEM design, the energy resolution of $b \leq 6\%\sqrt{GeV} / \sqrt{E}$ can be achieved with LKr averaged over the length of the barrel. This includes ~ 1.5 X_0 of inactive material in front of the active region. The pointing (angular) resolution with the segmentation as in Fig. 9 improves to $39 / \sqrt{E}$ mrad from $54 / \sqrt{E}$ mrad for the test device (Section 3.3 and Table I). A test of a module according to Figs. 9 and 10 is being prepared.

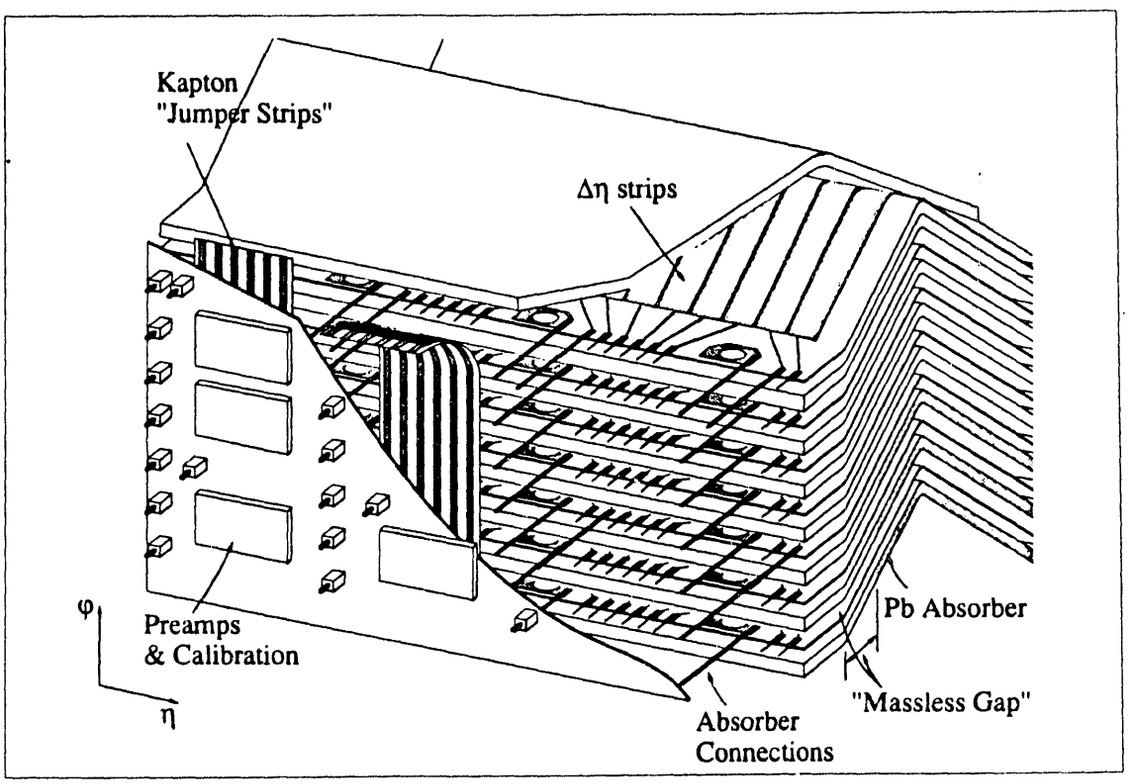

Fig. 10 Conceptual view of the electrode structure and connections of the calorimeter with a segmentation as in Fig. 9. The narrow strips are interconnected in ϕ by a flexible kapton board ("jumping strips"). A "massless gap" is realized by replacing lead in the absorber electrodes by a lower-Z material (e.g., G10).

Acknowlegement

We would like to thank the RD3 collaboration and in particular Daniel Fournier for many useful discussions. We would also like to thank the KEDR collaboration for providing the supply of krypton. This research was supported in part by the U.S. Department of Energy under contract DE-AC02-76CH 00016, and the National Science Foundation.

References

1. D. Axem, et al., The Lead-Liquid Argon Sampling Calorimeter of the SLD Detector, SLAC-PUB-5354 (1992)
2. B. Andriev et al., The H1 Liquid Argon Calorimeter, DESY-93-047 (1993)
3. S. Abachi et al., Nucl. Instr. and Methods A324, (1993)53; and H. Aihara et al., Nucl. Instr. and Methods A325 (1993) 393.
4. V. Radeka and S. Rescia,Nucl. Inst. and Methods A265 (1988) 228
5. SSC Detector R&D at BNL, BNL Report 52255, p.15 (1990)
6. B. Aubert et al., Nucl. Instr. and Methods A309(1991)438.
7. B. Aubert et al., Nucl. Instr. and Methods A321 (1992) 467.
8. B. Aubert et al., Nucl. Instr. and Methods A325 (1993) 116.
9. Aulchenko et al., Nucl. Instr. and Methods, A289 (1990) 468
10. F.D. Barr, Nucl. Instr. and Methods A323 (1992) 393
11. V. Aulchenko et al., Nucl. Instr. and Methods A327 (1993) 193.
12. O. Benary et al., "Performance of an Accordion Electromagnetic Calorimeter with Liquid Krypton and Argon," BNL-49536, submitted to Nucl. Instr. and Methods.
13. O. Benary et al., Nucl. Instr. and Methods, A332 (1993) 78.
14. O. Benary et al., "Liquid Ionization Calorimetry with Time-Sampled Signals," submitted to Nucl. Instr. and Methods.
15. GEM experiment Technical Design Report, GEM TN-93-262 (1993) unpublished.
16. O. Benary, W. Cleland, I. Ferguson, A. Gordeev, H. Gordon, E. Kistenev, P. Kroon, M. Leltchouk, D. Lissauer, H. Ma, D. Makowiecki, A. Maslennikov, S. McCorkle, D. Onoprienko, A. Onuchin, Y. Oren, V. Panin, J.A. Parsons, V. Radeka, L. Rogers, D. Rahm, S. Rescia, J. Rutherfoord, M. Seman, M. Smit, J. Sondericker III, R. Steiner, D. Stephani, E. Stern, I. Stumer, H. Takai, H. Themann, Y. Tikhonov, W. J. Willis, (The EM Liquid Ionization Calorimeter Collaboration of GEM.)
17. InterFET Corporation, 322 Gold Street, Garland, Texas 75042.
18. B. T. Turko and R. C. Smith, Proceedings of the 1991 IEEE Nuclear Science Symposium, Nov 2-9, 1991, p. 711.
19. W. E. Cleland and E. G. Stern, "Signal Processing Considerations for Liquid Ionization Calorimeters in a High Rate Environment," submitted to Nucl. Instr. and Methods, 1993.
20. H. Ma, "Performance of the GEM EM Calorimeter," these proceedings, p.

DATE
FILMED
4/28/94
END